The Abdus Salam
International Centre for Theoretical Physics

United Nations
Educational, Scientific
and Cultural Organization

International Atomic
Energy Agency

SMR.1771 - 6

Conference and Euromech Colloquium #480

on

High Rayleigh Number Convection

4 - 8 Sept., 2006, ICTP, Trieste, Italy

From convection in a closed cavity, Nu~Ra**1/3 limit, to convection in an open ended cavity, Nu~Ra**1/2 limit

J. H. Arakeri
Indian Institute of Science
Bangalore
India

Available online at www.sciencedirect.com
SCIENCE DIRECT®
ELSEVIER
International Journal of Heat and Mass Transfer 48 (2005) 4467–4473
International Journal of HEAT and MASS TRANSFER
www.elsevier.com/locate/ijhmt

Experiments and a model of turbulent exchange flow in a vertical pipe

Murali R. Cholemari, Jaywant H. Arakeri *

Department of Mechanical Engineering, Indian Institute of Science, Bangalore 560012, India

Received 27 December 2004; received in revised form 6 April 2005
Available online 19 July 2005

Abstract

In this paper we present experimental measurements of buoyancy driven turbulent exchange flow in a vertical pipe (L/d ratios of 9–12). The flow is driven by an unstable density difference across the ends of the pipe, created using brine and distilled water. Away from either end, a fully developed region of turbulence exists with a linear density gradient. Using a mixing length model that accounts for the end effects, we obtain the turbulent scales and flux. The Nusselt number scales like the square root of the Rayleigh number ($Nu \sim Ra^{1/2}$). We give an empirical relation to quantify the end effects and hence calculate the flux of the salt (NaCl) given the aspect ratio of the pipe and the overall density difference across it.

Keywords: Turbulent mixing; Exchange flow; Mixing length model

1. Introduction

This paper is concerned with turbulent natural convection in a long vertical pipe subject to an unstable density difference across the two ends. In the present paper we model the main mechanism that drives the turbulent flow, validate the model with experimental measurements and extend it to general cases. We discuss the implications of the model on the behaviour of the flux described in terms of a Nusselt number.

Fig. 1 shows the schematic of the flow. The pipe is connected by two tanks, with the top tank fluid having higher density than the bottom tank fluid. The two fluids are miscible. The incompressibility of the fluids implies that the cross section average of the axial velocity at any instant was zero. *This type of flow—where the net* flow is zero—is termed 'exchange flow' [1,2].

Most of the earlier work on exchange flow [1,2] has been in the context of the fire safety of buildings. Two types of studies have been done of flow through vent(s) connecting two enclosures, one above the other. One is flow due to the combined action of pressure and density differences across the vent, for example, as discussed in Tan and Jaluria [2], and the other type is due to density difference alone, for example as studied in Epstein [1]. The present flow is related to the latter type. Epstein [1] experimentally studied the buoyancy driven exchange (counter-current) flow through single or multiple openings with both square and circular cross sections in horizontal partitions, using brine above the partition and fresh water below the partition. The openings were tubes,

* *Corresponding author.* Tel.: +91 80 293 3228; fax: +91 80 360 0648.
E-mail address: jaywant@mecheng.iisc.ernet.in (J.H. Arakeri).

0017-9310/$ - see front matter © 2005 Elsevier Ltd. All rights reserved.
doi:10.1016/j.ijheatmasstransfer.2005.04.025

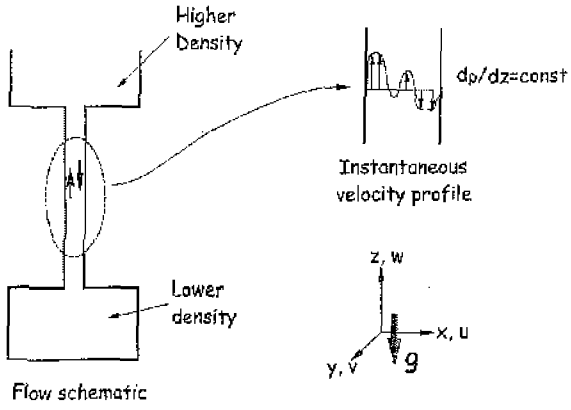

Fig. 1. Flow schematic, and a typical instantaneous axial velocity profile. The axial velocity averages to zero over the cross section at any given instant. The averages at any point over time of the velocities are zero as well.

projecting into the enclosures. The L/d ratios of the tubes were in the range 0.01–10. With a single opening, four different flow regimes were identified as L/d and $\Delta\rho$ were changed: a regime where an oscillatory exchange flow takes place which could be approximately explained by a linearized Taylor-wave theory (regime I), a Bernoulli flow regime where the dynamics is well explained by an inviscid exchange flow model by the application of the Bernoulli theorem [3] (regime II), and at the largest L/d ratios the exchange can be explained by turbulent diffusion, after Gardener [4] (regime IV). The combined effects of turbulent diffusion and Bernoulli flow are observed in regime III, which is modeled as Bernoulli type of flow at the ends of the tube and as a turbulent diffusion at the center of the tube. The peak mixing rate occurs in regime III. A different behaviour at each opening was observed when multiple openings were present. The analysis of this paper covers regimes III and IV.

Arakeri et al. [5] have studied the exchange flow in vertical pipes. The flow is driven by density difference across the pipe created using brine and fresh water. In different experiments, various combinations of pipe diameter and length are used to get a range of Rayleigh number $Ra = g(\Delta\rho/\rho_0 L)d^4/\nu\alpha$ from about 10^5 to 10^8. Using flow visualization, they identified four types of flow as a function of the Rayleigh number. At low Rayleigh numbers the flow is laminar, half-and-half (up and down flowing fluids are side by side). As the Rayleigh number is increased, a helical structure is observed, with the up and down-flowing fluids now forming a double helix. At still higher Rayleigh numbers the flow becomes unsteady, but still remains laminar. Finally beyond about $Ra = 10^7$, the flow was seen to be turbulent with a range of scales. They measured the average salt concentration in the top tank as a function of time and related the rate of change of the average concentration to the average flux of the salt in the pipe. For the turbulent flow, they developed a mixing length model with the length as the diameter of the pipe. In the turbulent case, the measured flux scaled like $\Delta\rho^{3/2}$ as predicted by the model. The laminar flux was higher than the turbulent flux. The convoluted paths in the turbulent flow taken by the fluids from either tank while flowing past each other and the mixing results in the lower flux in the turbulent case.

In the present study, we consider only the turbulent exchange flow which occurs at $Ra > 1 \times 10^6$. We concentrate on flux scaling for the exchange turbulent flow in large AR vertical pipes; the detailed structure of the turbulence is described in Cholemari [6]. We include in the analysis the effects of the developing flow at the pipe ends. We report experiments measuring both the density and the velocity fluctuations.

The aspect ratio AR (length-to-diameter ratio, L/d) of the tube was between 9 and 12. We used brine and distilled water for creating the density difference. The ratio of the diffusivities of momentum and salt, given by the Schmidt number, $Sc = \nu/\alpha$, is about 670, with ν and α being the kinematic viscosity of water and the diffusivity of salt respectively. The Rayleigh number, $Ra = g(\Delta\rho/\rho_0 L)d^4/\nu\alpha$, was of the order of 10^8, where $\Delta\rho$ is the density difference between the top and the bottom tanks, ρ_0 is the density of water and g is the acceleration due to gravity. This definition of Ra involving L and d is appropriate for this problem.

For the turbulent flow we found that the time means of the axial and lateral components of the velocities at each point were zero [6]. Thus there is no mean flow and no mean shear which implies that turbulence production is only due to buoyancy and none due to shear. Away from the ends of the pipe the turbulence was fully developed, or homogeneous in the axial direction. In particular, it can be shown that in the fully developed region the gradient of density is linear. The flow is driven by a linear unstable density gradient.

The rest of the paper is organized as follows. In Section 2 we describe the experiments conducted. Next (Section 3) we describe the modeling of the turbulence using the mixing length type arguments. Using experimental data we then extend the model to include the effects of the ends, and determine the prefactor in case of the flux scaling. We discuss the flow in relation with the Rayleigh–Bénard convection and conclude.

2. Experiments

Experiments were done to produce turbulent convection in long vertical glass pipes, and measure the flow characteristics. We visualized the flow and measured the velocities in the mid-section of the pipe, and the overall flux of salt within the pipe.

The setup (Fig. 2) essentially was a 50 mm diameter glass pipe connecting two tanks TT (Top) and BT (Bottom). The flow is visualized through a rectangular water filled glass tank surrounding the pipe to minimize refraction errors. To prevent stratification in the tanks, the fluid in each tank is continuously mixed. A small aquarium pump P circulated the fluid in each tank; heavier fluid was withdrawn from the bottom of the tank and re-introduced near the top of the tank through perforated pipes (PP). The fluid coming out of PP mixes with the surrounding fluid as it flows down, preventing stratification with minimal disturbance to the flow. The continuous mixing of fluids in the two tanks gives a well defined boundary condition at the two pipe ends.

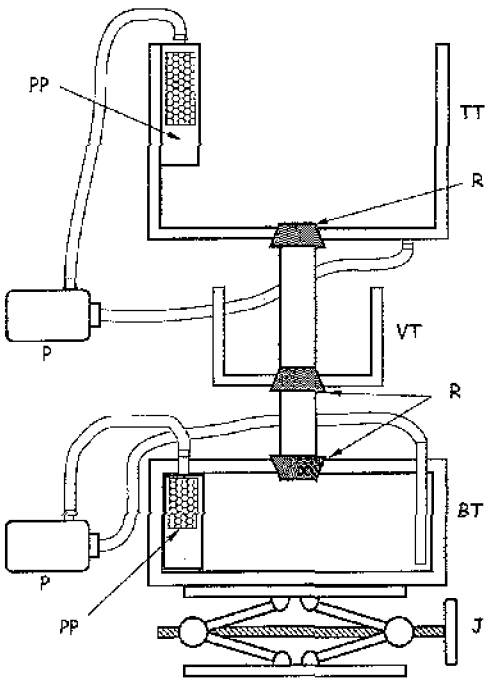

Fig. 2. Schematic of the experimental set-up; see text for notation.

Initially the top tank contains brine while the bottom tank and the pipe contain distilled water. A stopper separates the two fluids; the experiment is initiated by removing the stopper. Once the experiment is started, the fluids from the two tanks mix due to the flow in the pipe, continuously reducing the density difference. The flow thus slowly decays. Typical experiments lasted about three hours, but the flow was turbulent only for about the first 100 min. In our experiments the values of Ra varied from 5×10^8 down to 5×10^7. However the flow was turbulent for Ra larger than 1×10^8. The data considered for this paper is from the turbulent regime.

The flow visualizations (Fig. 3) indicate the flow to be random and three dimensional, with a high rate of mixing. The flow images are from the central homogeneous region, and are visualized with a 1.4 mm thick laser sheet. The process within the pipe is one of overturning and mixing and there is no mean flow. As mentioned above, the mean shear is thus negligible and buoyancy is the only source of turbulent kinetic energy. The pipe wall just contains the flow and has no role in the production of turbulence. The images also show the flow

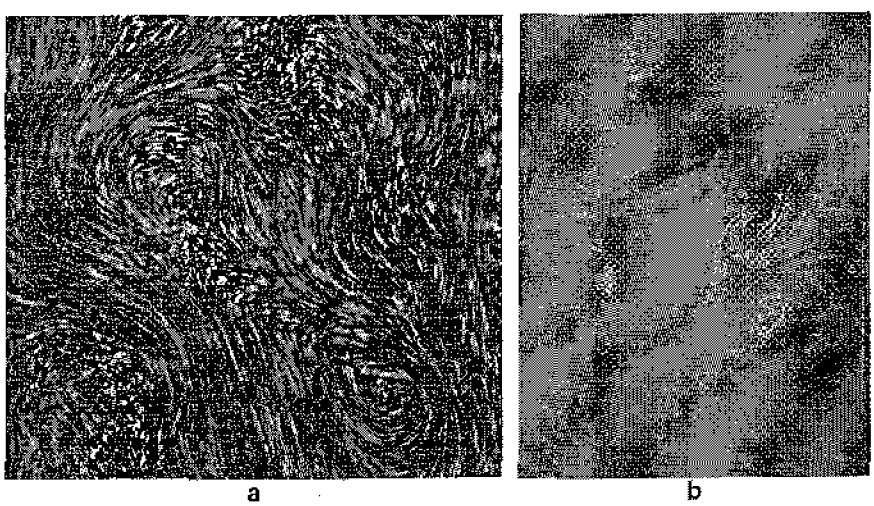

Fig. 3. (a) Particle streak image at $Ra \sim 2.5\times10^8$ and (b) Fluorescence dye visualization at $Ra \sim 1\times10^8$. The images show the flow to be random and to consist of a range of velocity scales (as seen in a range of streak lengths in (a)) and concentration scales (shown by the variation of image brightness in (b)). The area visualized is 50 mm × 50 mm in (a) and 50 mm × 67 mm in (b). The pipe is vertical in the images.

Table 1
Specifications of diagnostics used in the experiments

Technique	Spatial results	Temporal results	Dynamic range	Error
PIV	1.6/3.2 mm[a]	1 s	1–50 mm/s	~0.5 mm/s
Probe	NA	40 s	1.2–13.3 g/l	0.1% FSD

[a] 1.6 mm with 50% overlap.

to consist of a range of velocity and concentration scales.

We measured velocities at the middle of the pipe in the axial plane using planar Particle Image Velocimetry (PIV) and the salt concentration in the top tank using a conductivity probe (ORION SENSORLINK, model PCM100). Pipes of aspect ratios 9, 12 and 15 were used in the salt concentration experiments, while the velocity measurements were done with the $AR = 9$ pipe. The initial concentration of salt in the top tank was always 10 kg/m^3, corresponding to an Atwood number $At = (\rho_T - \rho_B)/(\rho_T + \rho_B) = 0.0035$. Table 1 gives the summary of the diagnostics. The details of the experiments are in Cholemari [6].

Knowing the rate of variation with time of the salt concentration in the top tank, we can calculate the concentration difference ΔC and the flux of the salt concentration F using an integral balance of the mass of the salt within the pipe;

$$C_B(t) = \frac{M_S - C_T(t)(V_T + V_P/2)}{V_P/2 + V_B} \tag{1}$$

$$\Delta C(t) = C_T - C_B = \frac{C_T(t)(V_T + V_B + V_P) - M_S}{V_P/2 + V_B} \tag{2}$$

$$F = \rho_0 V_T \, dC_T/dt \tag{3}$$

In the above, C_T and C_B are the top and bottom tank concentrations and ΔC the concentration difference; V_T, V_B and V_P refer to the volumes of the top and bottom tanks and the pipe, respectively; A_P is the cross sectional area of the pipe and M_S is the total mass of the salt in the set up. The concentrations are related to the density by,

$$\frac{\partial \rho}{\partial C} = \rho_0 \beta$$
$$\Delta \rho = \rho_0 \beta \Delta C$$
$$\rho = \rho_0 + \Delta \rho = \rho_0 + \rho_0 \beta \Delta C \tag{4}$$

where ρ_0 is the density of water and $\beta = 0.72$ for the salt concentration range encountered in the experiments. $\Delta\rho$ is the density difference between the top and bottom tank fluids.

Fig. 4 gives the flux of salt against the concentration difference. The inset gives the variation with time of the

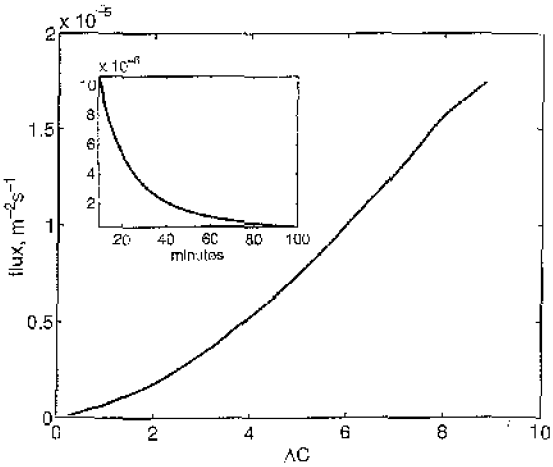

Fig. 4. Plot of the measured salt flux versus the salt concentration difference. Flux versus time is shown in the inset.

average top tank concentration. It is seen that the overall variation of the flow is slow. Typically an experiment lasts for about 100 min. The flow could thus be considered quasi-steady for periods of a few minutes.

3. Model

We now show that the fully developed turbulence in the central region can be described in terms of a single length scale, the diameter of the pipe. The flux of salt, the fluctuations of velocity and the salt concentration are given by this description to within prefactors. The flow at the pipe ends is expected to be different. We extend the mixing length arguments to include the end effects. This enables us to obtain the prefactor in the flux relation as well as to give a relation for the salt flux in terms of the aspect ratio, the overall density difference between the two tanks and the pipe diameter.

For a long enough pipe ($L/d \gg 1$), away from the two ends the flow must be homogeneous in the axial direction with a linear density gradient. The present flow may be compared with the fully developed pressure driven pipe flow. In the latter, the flow is homogeneous (away from the entrance) in the axial direction and driven by a linear pressure gradient; in the present flow, the homogeneous flow is driven by a linear (unstable) density gradient.

First we consider the central homogeneous region. The only relevant parameters are the pipe diameter, d, the density gradient, $d\rho/dz$, g, ν and α. The two molecular parameters ν and α are not relevant for a turbulent flow. Then dimensional analysis gives the scales for density fluctuations ρ', velocity fluctuations w' and salt flux $-\alpha\frac{\partial C}{\partial z} - \langle wc \rangle \simeq -\langle wc \rangle$ as

$$w' \sim \sqrt{g(\partial\rho/\partial z)d^2/\rho_0} = w_m \tag{5}$$

$$\rho' \sim (\partial\rho/\partial z)d = \rho_m \tag{6}$$

$$\frac{w_m\rho_m}{\beta\rho_0} = F_m \tag{7}$$

where w_m, ρ_m and F_m are the mixing length scalings for the fluctuations of velocity and density and the flux of salt respectively. Thus we may write the flux F as

$$F = C_m F_m = C_m \frac{\sqrt{g/\rho_0}(\partial\rho/\partial z)^{3/2}d^2}{\beta\rho_0}. \tag{8}$$

The constant C_m needs to be determined from the experiments.

Physically, the scales may be interpreted as follows. A coherent region of fluid (a fluid particle) scales with the pipe diameter in the fully developed region. The velocity scale can be can be thought as a 'free fall' velocity of the fluid particle heavier (or lighter) than the surrounding fluid by an amount ρ' falling (or rising) through a distance d, i.e., the length over which the correlation exists.

There would be a development region near the pipe ends with non-linear density gradient (Fig. 5) where the distance from the pipe ends would become important in addition to the pipe diameter. Because of the non-linear density gradient, the (unknown) linear density gradient at the central region would be different from $\Delta\rho/L$ (i.e., $\partial\rho/\partial z \neq \Delta\rho/L$).

The parameters relevant to the end regions are L_e, the extent of end region, and $\Delta\rho_e$, the density drop at the ends (see Fig. 5). For a turbulent flow these parameters depend only on the flux and the diameter, as the molecular parameters are not important. The flux is the same throughout the pipe. From (8) we see that flux depends on $(\partial\rho/\partial z)$ and d. Thus $\Delta\rho_e$ and L_e are the functions of the parameters at the central region, viz. $\partial\rho/\partial z$ and d. Thus, from dimensional analysis

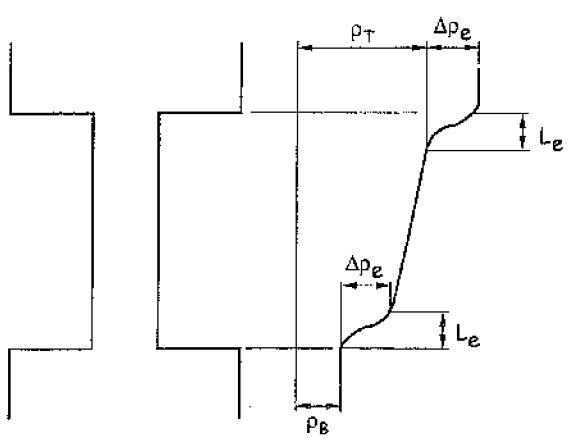

Fig. 5. Schematic of the end regions. The density drops by $\Delta\rho_e$ over a distance L_e. The density variation is non-linear.

$$\Delta\rho_e = k_\rho \frac{\partial\rho'}{\partial z} d,$$

$$L_e = k_L d. \tag{9}$$

Thus,

$$\frac{\frac{\partial\rho}{\partial z}}{\Delta\rho/L} - \left(\frac{1-2L_e/L}{1-2\Delta\rho_e/\Delta\rho}\right) = \frac{1}{1+2(k_\rho - k_L)/AR}. \tag{10}$$

The flux is then given by

$$F = C_m \frac{(g/\rho_0)^{1/2}d^2}{\beta\rho_0}\left(\frac{\partial\rho}{\partial z}\right)^{3/2} - C_r \frac{(g/\rho_0)^{1/2}d^2}{\beta\rho_0}\left(\frac{\Delta\rho}{L}\right)^{3/2}, \tag{11}$$

with,

$$C_r = \frac{C_m}{\left(1+2(k_\rho - k_L)/AR\right)^{3/2}}. \tag{12}$$

In the limit of large AR, the entry regions become negligible in comparison with the length of the tube and $C_r \to C_m$. Fig. 6(a) shows the experimentally obtained values of C_r in the experiments of [1,5,7]. Also shown is the fit for the data for $AR > 3$, where a fully developed region is expected to exist at the center, shown as filled symbols. The fit constants are

$$C_m = 0.88 \tag{13}$$

and

$$k_\rho - k_L = 2.1. \tag{14}$$

With these values, (12) becomes,

$$C_r = \frac{0.88}{(1+4.2/AR)^{3/2}}. \tag{15}$$

The fit extended towards smaller AR is shown as the dashed line. It compares quite well with the experimental data even at small AR where the assumption of the existence of a central homogeneous region will not be valid. Velocity measurements near the ends indicate that there is a development region of about one diameter and so we can take $k_L = 1$ which implies $k_\rho = 3.1$, which means that the density drop at the pipe ends is about three times the density drop over one diameter length in the central region. The presence of the end regions reduces the linear density gradient in the centre of the pipe and hence the flux. It follows from Eqs. (9) and (10)

$$\frac{\Delta\rho_e}{\Delta\rho} = \frac{k_\rho}{AR + 2(k_\rho - k_L)},$$

$$\frac{L_e}{L} = \frac{k_L}{AR} \tag{16}$$

These parameters are plotted in Fig. 6(b). It is seen that by about $AR = 10$, the end regions extend only to about 10% of the pipe length at each end, but they account for about 40% of the total density drop across the pipe. These reduce to respectively 5% and 25% by $AR = 20$.

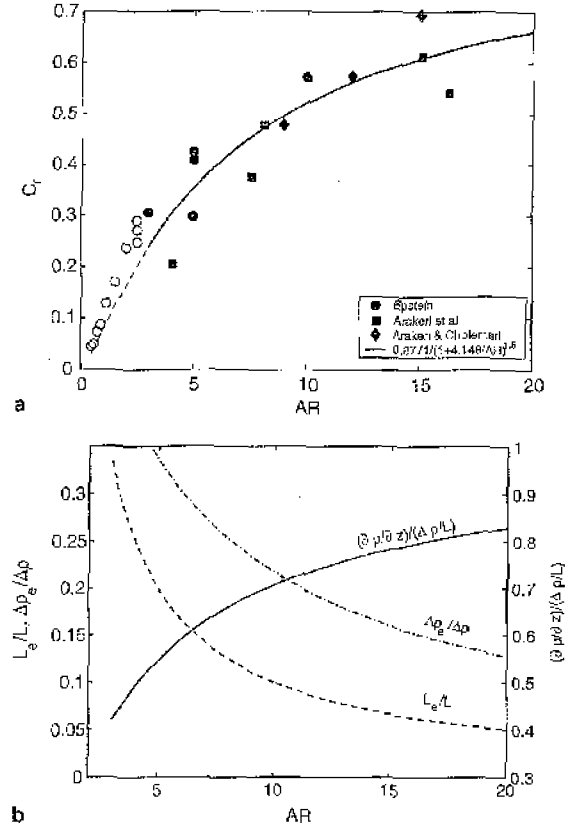

Fig. 6. (a) C_r from experiments (filled symbols), and the model fit (shown as solid line) against the aspect ratio L/d. The dashed line is the extension below $L/d = 3$ (clear symbols). (b) End effects calculated according to the model. Shown are the fraction of the total concentration drop occurring at either end ($\Delta\rho_e/\Delta\rho$) as well as the extent of the region (L_e/L).

C_m, the mixing length prefactor, is expected to be independent of the specific conditions of the flow, like AR, $\Delta\rho/\rho_0$, etc., and is expected to hold when the conditions of a single length scale and the linear density gradient are met.

To compare Eq. (15) with the results of Epstein [1], we note that, Eq. (22) in that paper, when written similar to Eq. (11), shows

$$C_r = \frac{4/\pi \times 0.093}{\left[AR^{-3} + 0.084(1 - 0.4/AR)^3\right]^{1/2}}. \tag{17}$$

The mixing length prefactor calculated from (17) in the limit of large AR, $C_r \to C_m = 4/\pi(0.093/\sqrt{0.084}) = 0.41$. We surmise that the data leading to Eq. (22) in Epstein consists in part of non-turbulent data, leading to the deviation from (13).

The flux relation (11) written in terms of the Nusselt number (the non-dimensional flux), and the Reynolds number using w' ($\sim w_m$) and d have the following scalings with the Rayleigh number:

$$Nu = -\frac{< flux >}{\alpha\Delta C/L} = C_r Ra^{1/2} Sc^{1/2}, \tag{18}$$

$$Re = \frac{w'd}{\nu} \sim Ra^{1/2} Sc^{-1/2}. \tag{19}$$

Note also that $Nu \to C_m Ra^{1/2} Sc^{1/2}$ for very large AR, which is another way of looking at Eq. (18) when the Nusselt number is defined using the density difference over a certain length say, one diameter, in the linear gradient region.

Fig. 7(a) compares the rms velocities obtained from PIV measurements to the velocity scale obtained from

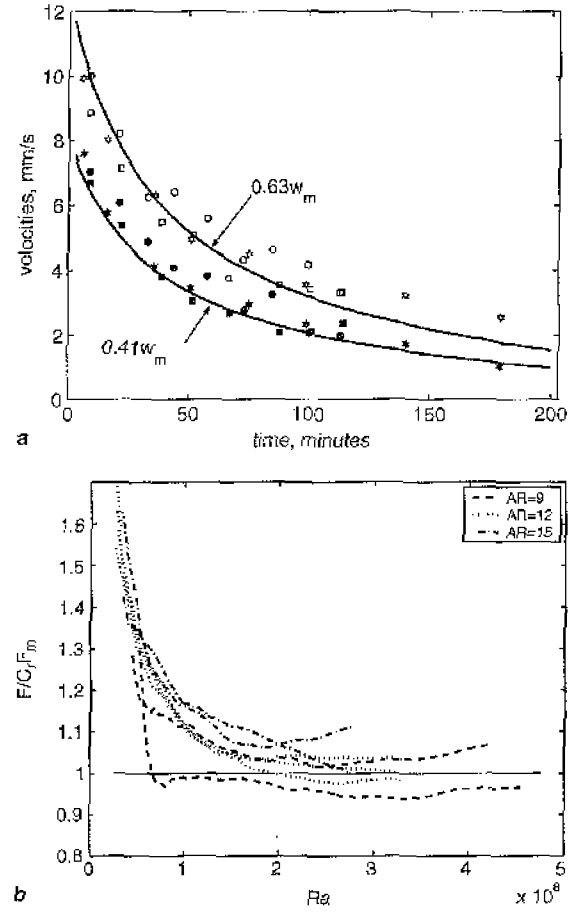

Fig. 7. (a) Velocity scaling according to the mixing length model (lines), compared with the measured velocities (filled symbols—lateral velocity, open symbols—axial velocity). (b) Flux of salt normalized with the flux according to the mixing length model, $C_r F_m$. The constant regions during the experiments shows the validity of the hypothesis. The pipe diameter is 50 mm.

the model using the density measurements (Eqs. (5) and (4)) in the top tank. Here the average of the RMS velocity calculated over every 10 min over the pipe cross section area is plotted with time. It is seen that the scaling is good for the regime under consideration, both the axial and lateral velocities following the mixing length scaling w_m. However beyond about 100 min when the flow is no longer turbulent, the agreement is poor. Fig. 7(b) shows the turbulent flux normalized with the flux obtained from the model (Eq. (11)). The value is constant and within 10% of unity for an extended range of the Rayleigh number. However, at lower Rayleigh numbers below 1×10^8, the turbulent scaling is not appropriate and the normalized fluxes rise sharply above unity. The flow is not turbulent for $Ra < 2 \times 10^8$.

The overall uncertainty in the measured flux scaling is obtained from Eq. (8) as

$$\frac{\epsilon_F}{F} = \frac{3}{2}\frac{\epsilon_{\Delta\rho}}{\Delta\rho}. \tag{20}$$

The worst case is at the smallest density differences, where the error is about 1.5% (see Table 1).

The Nusselt number relation (18) is of the same form as the theoretical expression of Kraichnan [8], for Rayleigh–Bénard (R–B) convection at very high Rayleigh numbers of the order of 10^{18}, where the flow mechanics is expected to be dominated by the processes in the bulk of the flow, away from the walls. However, no experimental evidence for the $Ra^{1/2}$ regime is seen in R–B convection, even at very high Rayleigh numbers of about 10^{17} achieved so far in the experiments [9]. An important difference between the two types of flows is that, in R–B convection, even at high Rayleigh numbers, boundary layers exist near the two horizontal walls and have an effect on the flow, whereas in the present flow boundary layers are absent.

It can be shown that the flux obtained for a given density difference in the present flow is much higher than the flux in R–B convection at the same density difference. To do this, we first obtain the prefactor in Eq. (18) to be 0.0752 at unit aspect ratio (as we want to compare with R–B convection which is at about unit aspect ratio or lower) using Eq. (12). Nusselt number at $Ra = 10^8$ and $Sc = 670$ then turns out to be ~1950. To obtain a similar estimate in case of R–B convection, we use the experimental correlation of Globe and Dropkin [10], $Nu \sim 0.097 Ra^{1/3}$. This is for a Prandtl number of 100, but we assume its validity for $Pr = 670$ and estimate the Nusselt number at the same Rayleigh number to be much smaller, ~45.

4. Conclusion

In this paper we have described a purely buoyancy driven turbulent flow in long vertical pipes, with a fully developed region of turbulence with an unstable linear density gradient. Using a mixing length theory and dimensional arguments, we have developed a relation for the flux in the present turbulent convection. The analysis includes the effects of the ends. Experimental results have been used to validate the predicted scaling and to obtain values of the constants in the flux relations. Eq. (11) with C_F determined empirically in (15) is the relation for the flux. The flux is a function of the concentration difference, the pipe length and the aspect ratio. The scaling relations for the velocity fluctuations are well predicted by the model (Eq. (5) and Fig. 7(a)). This is of use in design practice, for example, when air fluxes need to be calculated across a staircase connecting rooms with different temperatures.

The mixing length model implies the Nusselt number to scale as $\sim Ra^{1/2}$, in contrast to R–B convection for similar Rayleigh numbers as in the present flow, where it goes like $\sim Ra^n$, with $2/7 < n < 1/3$. The absence of the top and bottom horizontal walls and the associated boundary layers in the present flow mainly accounts for this large difference.

References

[1] M. Epstein, Buoyancy driven exchange flow through small openings in horizontal partitions, J. Heat Transfer 110 (1988) 885–893.

[2] Q. Tan, Y. Jaluria, Mass flow through a horizontal vent in an enclosure due to pressure and density differences, Int J. Heat Mass Transfer 44 (2001) 1543–1553.

[3] W.G. Brown, Natural convection through rectangular openings in partitions—2: horizontal partitions, Int. J. Heat Mass Transfer 5 (1962) 869–881.

[4] G.C. Gardener, Motion of miscible and immiscible fluids in closed horizontal and vertical ducts, Int. J. Multiphase Flow 3 (1977) 305–318.

[5] J.H. Arakeri, F.E. Avila, J.M. Dada, R.O. Tovar, Convection in a long vertical tube due to unstable stratification – a new type of turbulent flow? Current Sci. 79 (6) (2000) 859–866.

[6] M.R. Cholemari, Buoyancy driven turbulence in a vertical pipe, Ph.D. thesis, Department of mechanical engineering, Indian Institute of Science, 2004.

[7] J.H. Arakeri, M.R. Cholemari, Fully developed buoyancy driven turbulence in a tube, in: Proceedings of the 9th Asian Congress Fluid Mech., Isfahan University of Tech., Iran, 2002.

[8] R.H. Kraichnan, Turbulent thermal convection at arbitrary Prandtl number, Phys. Fluids 5 (11) (1962) 1374–1389.

[9] J.J. Niemela, L. Skrbek, K.R. Sreenivasan, R.J. Donnelly, Turbulent convection at high Rayleigh numbers, Nature 404 (2000) 837–841.

[10] S. Globe, D. Dropkin, Natural convection heat transfer in liquids confined by two horizontal plates and heated from below, ASME J. Heat Transfer 81 (1959) 24–28.

Convection in a long vertical tube due to unstable stratification – A new type of turbulent flow?

Jaywant H. Arakeri*,§, Fransisco E. Avila†, Jorge M. Dada and Ramon O. Tovar

*Department of Mechanical Engineering, Indian Institute of Science, Bangalore 560 012, India
Centro De Investigacion en Energia, Temixco, UNAM, Mexico

We present experimental results of free convection in a vertical tube due to an unstable density difference imposed between the two (open) ends of the tube. Two tanks of fluids connect the two ends of the tube with the top-tank fluid heavier than the bottom-tank fluid. We use salt mixed with water to create the density difference. The convection in the tube is in the form of relatively heavier fluid going down and lighter fluid going up simultaneously; the mean flow at any cross section of the tube is zero. Depending on the Rayleigh number we observe different types of flow, with turbulent flow being observed at the higher Rayleigh numbers. We believe this is a new type of turbulent flow – a nearly homogeneous, buoyancy-driven flow with zero mean shear.

FLOWS caused by buoyancy, called free or natural convection, abound in nature and engineering. The convection observed on a hot road surface in no-wind conditions is an example. Convection is generally caused by unstable stratification (for example, density increasing with height in a gravitational field). Density gradients are often caused by a temperature gradient, or a gradient of concentration of some species (e.g. salt in the oceans, water vapour in air). The dynamics in free-convection flows is mainly determined by the Rayleigh number – a measure of the ratio of buoyancy forces to diffusive effects.

Two simple configurations of free convection have been extensively studied, viz. Rayleigh–Benard convection and Rayleigh–Taylor instability. Rayleigh–Benard (R–B) convection is convection of a fluid between two horizontal plates, with the bottom plate hotter than the top plate. Because of the temperature difference, the fluid density increases from the bottom plate to the top plate. However, below a critical Rayleigh number, even though the stratification is unstable, there is no flow (convection) and heat transfer is entirely by conduction; the Rayleigh number increased beyond this critical value results in laminar convection, often in the form of rolls, and a further increase in the Rayleigh number leads to turbulent convection (see ref. 1).

§For correspondence. (e-mail: jaywant@mecheng.iisc.ernet.in)
†Sadly, Fransisco passed away during the writing of this paper. We have fond memories of him.

Rayleigh–Taylor instability occurs when a layer of heavier fluid (say salt water) lies on top of a layer of lighter fluid (say fresh water). Dalziel *et al.*[2] report recent work on this subject. In this configuration the layers can be in equilibrium; pressure varies linearly with depth in each of the layers. But this is unstable equilibrium: a small perturbation of the interface increases the perturbation indefinitely with the heavier fluid trying to go down and the lighter fluid trying to go up. Some mixing between the top and bottom fluids occurs during the overturning. Eventually motion ceases and a stable density gradient is obtained. For an immiscible pair of fluids of say water over air there is negligible mixing and, eventually, the water and air layers just interchange places. One common way of doing a Rayleigh–Taylor stability experiment is to have a thin plate initially separating the two fluids which is then rapidly pulled away.

In this article we describe preliminary results of free convection in a vertical tube. The setup is similar to a Rayleigh–Taylor stability setup, except that we have a long vertical tube between the tanks containing the heavier fluid at the top and the lighter fluid at the bottom (Figure 1). So essentially we look at the 'overturning' process of the two fluids through the tube. We used sodium chloride salt mixed in water to create the density difference. As in Rayleigh–Benard convection, we find different types of flow depending on the values of the parameters of the problem: the density difference, and diameter and length of the tube. In particular, at a high enough Rayleigh number we observe the flow to be turbulent, which we believe is a new type of turbulent flow.

Experimental setup

The experimental setup consisted of two tanks connected by a vertical tube. The top tank was open at the top and had a tapered hole in the bottom plexiglas wall to fit a rubber stopper; an appropriate sized hole was made in the stopper to snugly fit the tube. The bottom tank was closed on all sides and had a similar rubber stopper arrangement on the top wall to fit the bottom end of the tube. The rubber stoppers minimized the load

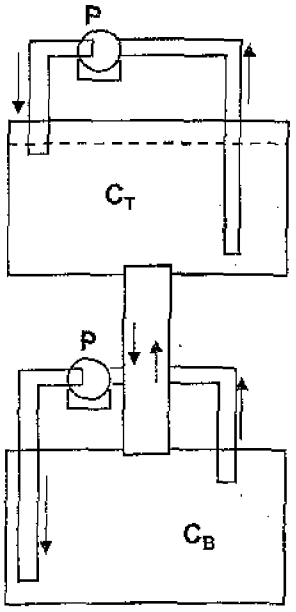

Figure 1. Schematic of the experimental setup. The pumps in the two tanks are marked P.

on the tubes, which were made of glass, and also allowed us to quickly change the tube for a different experiment. The side walls of the tanks were made of glass. Two small aquarium water pumps were used to continuously mix the fluids in the two tanks and prevent stratification. The flow rates in the pumps were small enough and the locations of the exits and inlets of the pumps were such as to create as small a disturbance as possible near the tube ends.

The volumes of the two tanks were approximately 1750 cc each. A total of twelve tubes were used in the experiments, with four diameters (4.85, 9.85, 19.85 and 36.85 mm) and three lengths (150, 300 and 450 mm). A few visualization experiments were conducted with 2.5 mm diameter tubes.

Following is the experimental procedure. We calibrated the conductivity probes, used to measure salt concentration, before and after each experiment. We filled the bottom tank and the tube with distilled water, and the top tank with brine (typically 0.05 g cm^{-3} concentration), noting down the volumes of the distilled water and brine added. We switched on the pumps prior to the start of each experiment. Initially, a stopper blocked the top end of the tube; pulling of the stopper initiated the experiment. Due to the convection the salt concentration in the top tank continuously decreased with time (Figure 2). Concentration in the top tank was measured from the start of the experiment till the convection had visibly stopped. In the smallest diameter and longest tube (4.85 mm dia, 600 mm long) the convection continued for about 100 h, whereas in the largest diameter tube the convection continued for about 1 h.

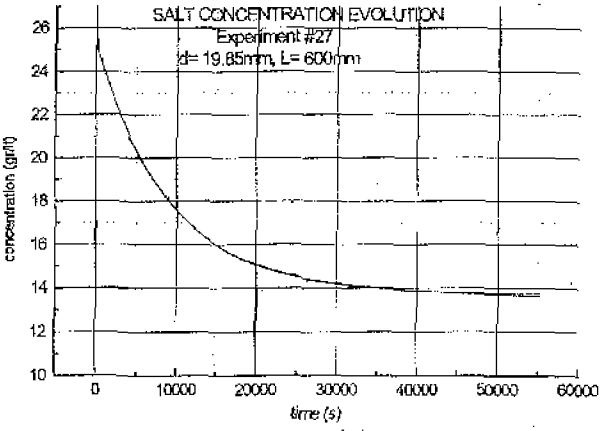

Figure 2. A typical variation of concentration of salt in the top tank fluid with time. The case shown corresponds to tube diameter = 19.85 mm and tube length = 600 mm.

Salt concentration was measured with one or two micro-conductivity probes (Model 125 MSCTI, Precision Measurements Engineering), placed in the top tank. The concentration versus time data were stored in a computer for further analysis. Two conductivity probes were used to check that mixing by the pump was adequate and there was no concentration gradient in the tank fluid. We mainly visualized the flow using the laser-induced-fluorescence (LIF) technique. A small amount of sodium fluorescent dye was initially mixed in the top tank fluid. A vertical sheet of laser light, created with a cylindrical lens, passed through the vertical tube (in which the convection was taking place). We used a 150 mW argon-ion laser. In some cases, we also visualized the flow using the shadowgraph technique.

Parameters

We are looking at free convection in a vertical tube open at the two ends, with an imposed density, or concentration, difference across it. As in Rayleigh–Benard convection, the non-dimensional parameters of the problem are:

$$\text{Rayleigh number, } \mathrm{Ra}_l = \frac{g\Delta C l^3}{\rho \nu \alpha},$$

$$\text{Prandtl number, } \mathrm{Pr} = \frac{\nu}{\alpha},$$

$$\text{Aspect ratio, } \mathrm{AR} = \frac{d}{l},$$

where ΔC is the concentration (or density) difference between the top tank and bottom tank fluids, ρ, is the density of the fluid averaged over the length of the tube, g is acceleration due to gravity, ν is the kinematic viscosity, α is the diffusivity of the species causing

the density gradient, d is tube diameter, and l is tube length.

Sometimes it is more appropriate to use other definitions of Rayleigh number: Ra_d, Rayleigh number based on the tube diameter, and Ra_G, Rayleigh number based on the density gradient, instead of density difference, and diameter.

Some values of the parameters are of interest. The Prandtl number, or strictly the Schmidt number, is about 670, showing diffusion of salt is negligible in comparison to that of momentum. At a concentration difference of 0.025 g/cm^3 and for a tube length = 600 mm, the Rayleigh number = 3.5×10^{13}. The AR ranges from about 0.008 to about 0.25. For comparison, study of turbulent Rayleigh–Benard thermal convection is usually with Pr ~ 1 (for air Pr = 0.7 and for water Pr = 6.7); the Rayleigh number is usually of the order of 1×10^8, but the highest value achieved, reported recently[5], using cryogenic helium is about 1×10^{17}; and AR is usually greater than unity. Thus the present problem pertains to very large Rayleigh number, high Prandtl number convection in tall cells. High Prandtl number, high Rayleigh number convection is generally obtained with very viscous fluids convecting over a large scale, as in convection in the earth's mantle.

Basic relations

From the salt concentration (in the top tank) versus time data we calculate the flux of salt, and the concentration difference between the two tank fluids as functions of time. This is done using mass conservation equations.

We use cylindrical polar coordinates (r, θ and z) with velocities in the three directions respectively, U_r, U_θ and W. The z-axis coincides with tube axis and is positive upwards. An overbar over a quantity denotes the quantity averaged over the cross-section of the tube. The difference between a quantity and its average is written in small case. Thus for concentration

$$\overline{C} = \int_A C \mathrm{d}A, \quad c = C - \overline{C}.$$

Fluid volumes in each of the two tanks do not change with time. Thus, at any cross-section of the tube and any instant of time (assuming water to be incompressible) the volume flow rate of the fluid going down = the volume flow rate of fluid going up, or

$$\int_A W \mathrm{d}A = \overline{W} = 0.$$

We come to the important conclusion that the mean velocity at any cross-section is zero.

The mass flow rate of salt $\dot{m}_s$ going up at any z is

$$\dot{m}_s = \int_A CW \mathrm{d}A = \overline{cw} A_p,$$

where A_p is the cross-sectional area of the tube. From mass conservation of salt at any z we have the gradient of $\dot{m}_s$,

$$\frac{\partial \dot{m}_s}{\partial z} = -\frac{\partial}{\partial t}\left(\int_A (C \mathrm{d}A) \right) = -A_p \frac{\partial \overline{C}}{\partial t}.$$

The equation states that in a control volume height dz, the difference in mass flow rates at two stations dz apart is equal to the rate at which mass of salt changes in the control volume. If $(\partial \overline{C}/\partial t) = 0$, then $\dot{m}_s$ is constant along the length of the tube; however, $\dot{m}_s$ can still be a function of time.

At any time let C_T and C_B be the concentrations of salt in the top and bottom tanks respectively, and C_{T0} and C_{B0} the concentrations at the start of the experiment. Mass conservation of salt gives

$$V_T C_T + V_B C_B + A_P \int_0^l \overline{C} \mathrm{d}z = V_T C_{T0} + V_B C_{B0} + A_P \int_0^l \overline{C}_0 \mathrm{d}z = M_s,$$

Where V_T and V_B are respectively the top and bottom tank fluid volumes, A_P is the pipe cross section area, and M_s is the total mass of salt in the system. The integral on the left-hand side is the mass of the salt in the tube. Assuming the average salt concentration in the tube at any time is $(C_T + C_B)/2$, we obtain the following relation for the concentration or density difference in terms of the concentration in the top tank:

$$\Delta C = (C_T - C_B) = C_T \frac{(V_T + V_B + V_P)}{(V_B + V_P/2)} - \frac{M_s}{(V_B + V_P/2)}, \quad (1)$$

where V_p is the volume of the tube.

Let $\dot{m}_{sT}$ be mass flow rate of salt at the top end of the tube and $\dot{m}_{sB}$ at the bottom end of the tube. Then

$$\dot{m}_{sT} = V_T \mathrm{d}C_T/\mathrm{d}t, \quad \dot{m}_{sB} = -V_B \frac{\mathrm{d}C_B}{\mathrm{d}t},$$

$$\dot{m}_{sT} - \dot{m}_{sB} = \frac{\mathrm{d}}{\mathrm{d}t} \int_0^l \overline{C} \mathrm{d}z.$$

The relations respectively are from salt mass conservation in the top tank, bottom tank and in the tube. In

our experiments, to a good approximation, we can assume

$$\dot{m}_{sT} = \dot{m}_{sD} = \dot{m}_s = V_T \frac{dC_T}{dt}.$$

Then flux, mass flow rate of salt going down per unit cross sectional area of the tube is,

$$F = -\overline{cw} = -\frac{V_T}{A_p}\frac{dC_T}{dt}. \quad (2)$$

Flow visualization observations

Depending on the concentration difference, the tube diameter and the tube length we observe one of four types of flow which we term (i) half-and-half (HAH), (ii) helical, (iii) unsteady-laminar and (iv) turbulent. These are described below. It may be noted that the flow visualization pictures given in this paper show just a few centimetres length of the central portion of the tube.

Half-and-half flow

In a HAH flow, in one half of the cross section of the tube flow is downward, and in the other half the flow is upward. We observed the HAH flow only in the 2.5 mm dia tube and in the 4.85 mm dia tube at small concentration differences, essentially meaning at low Rayleigh numbers. In some cases we observed moving fronts, about 1–2 tube diameters long. A downward moving front is heavier and moves faster than the rest of the down-going fluid; similarly an upmoving front is lighter than the rest of the up-going fluid. Figure 3 is a shadowgraph picture showing both down-going and up-going fronts.

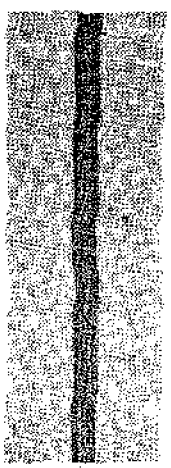

Figure 3. Shadowgraph picture showing two fronts in HAH convection. Tube diameter is 2.5 mm.

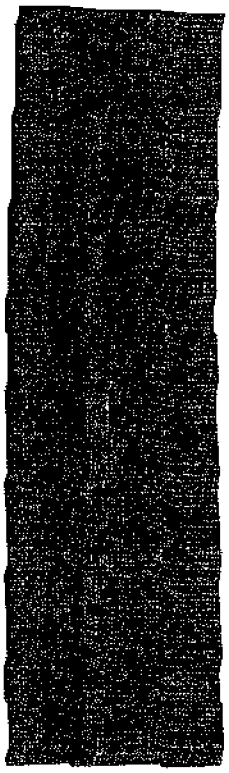

Figure 4. LIF picture showing helical convection. Tube diameter = 4.8 mm; tube length = 150 mm; concentration difference = 0.025 g/cc. Top-tank fluid is dyed. Only the central length of the tube is shown.

Helical flow

We observed helical flow in the 4.85 mm dia tube (Figure 4), except at small concentration differences when the flow was HAH (Figure 4). As in HAH flow the helical flow is equally divided between up-going and down-going fluid, and is steady. In HAH flow the interface between the up-going and down-going flows is vertical and straight; however, in helical flow the interface is twisted. The interface looks like what one would get if a long strip of paper is held at one end and the other end is turned through many turns; going along one edge of the strip one would trace an helix. Thus the two flows (up and down) take helical paths with a common (twisted) interface. In most cases we observe some mixing between the fluids in the two streams. Apparently the HAH flow is unstable above some (yet undetermined) critical Rayleigh number and the instability leads to helical flow.

Unsteady-laminar flow

In the 9.85 mm and 19.85 diameter tubes (i.e. at still higher Rayleigh numbers) we observe the flow to be unsteady and three dimensional, but laminar (Figures 5 and 6). There is no clear demarcation between the up-going and down-going flows, and there is a lot of mixing between the two. A typical mixing event involves collision of a downward going mass of fluid with a upward going mass of fluid, often leading to shear layers which go unstable with the formation of vortices. One also sees mushroom type structures (see Figure 5). The eddies seem to scale with the diameter of the tube. The flow is chaotic, but atleast in the 9.85 mm dia tube the flow is not turbulent: a range of scales, characteristic of turbulent flows is not present.

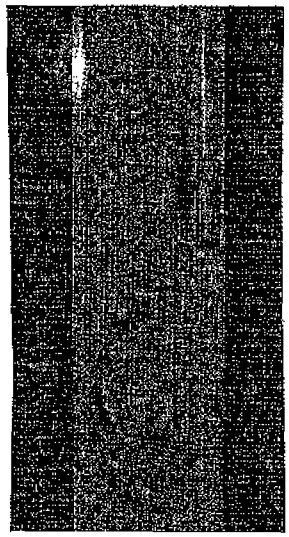

Figure 5. LIF picture showing unsteady-laminar convection. Note the mushroom structure. Tube diameter = 9.85 mm; concentration difference = 0.025 g/cc.

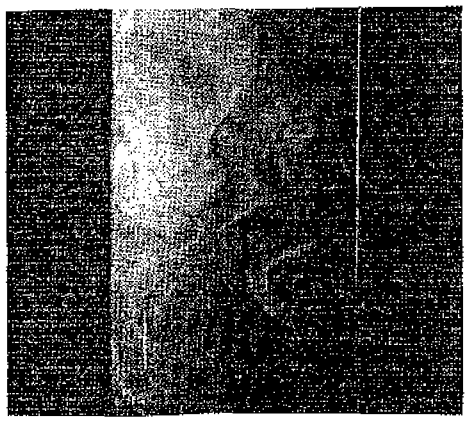

Figure 6. LIF picture showing unsteady-laminar convection. Tube diameter = 19.85 mm; Tube length = 300 mm; concentration difference = 0.025 g/cc.

Figure 7. LIF picture showing turbulent convection. Note the small length scales of mixing. Tube diameter = 37 mm; concentration difference = 0.025 g/cc.

Turbulent flow

What appears to be a truly turbulent flow is observed in the 36.85 mm diameter tube (Figure 7). Like in the 9.85 mm and 19.85 diameter tubes, the flow is chaotic and three dimensional. We observe collisions of fluid masses moving in opposing directions, and the formation and breakup of shear layers. During these interactions large interfacial areas are created greatly enhancing the mixing between the heavier and lighter fluids. Also because of collisions we can have instances when heavier masses of fluid move up instead of down, and similarly instances when lighter fluid masses go down. Both mixing and flow direction reversal contribute to reduction of flux, or in other words to slowing down of the experiment.

Flux relations

The flux times the tube cross sectional area, $-\overline{c\omega}A_p$, determines how fast the top tank depletes salt, or equivalently how fast the bottom tank accumulates salt. A large flux is obtained if all the down-going fluid ($w < 0$) has higher density ($c > 0$) (similarly when $w > 0$, c is < 0), and in addition if $|w|$ and $|c|$ are as large as possible. The maximum possible c is ΔC, when all the down-going fluid is pure top tank fluid and all the up-going fluid is pure bottom tank fluid; there is no mixing of the two in the tube. The maximum possible velocity is probably what is obtained by assuming half-and-half laminar flow, and whose solution is given below. Flux can be reduced due to two reasons. One, mixing between down-going and up-going fluids reduces the values of both c and w; two, heavier fluid moving down, or vice versa, reduces the correlation.

A trivial case is when there is no flow and the salt transfer is just by molecular diffusion; then flux is given by $F = \alpha\Delta C/l$. Stability analysis[4] shows that when the tube is thin enough or density difference small enough, or more precisely the gradient Rayleigh number $Ra_G < 1087$, there is no flow. (This analysis is for a density increasing linearly with height.) We never observed a no-flow case in any of our experiments as the Rayleigh number was above the critical value, except perhaps towards the end of an experiment when the density differences were too low to be measured by our instrumentation.

Next we derive expressions for the flux of salt in the vertical tube for two cases: (i) laminar half-and-half flow of immiscible fluids and (ii) turbulent convection.

Laminar HAH flow of immiscible fluids

Consider fully developed parallel flow in the vertical tube. We assume the heavier fluid (density = ρ_T) is going down in one half of the tube, say $\pi > \theta \geq 0$, and the lighter fluid (density = ρ_B) is going up in the other half, $2\pi > \theta \geq \pi$. Fluids in the two streams have same kinematic viscosity and are immiscible (equivalent to saying diffusivity of salt is zero). With U_r, $U_\theta = 0$ (parallel flow) and $d/dz = 0$ (fully developed flow), the Navier–Stokes equations simplify to

$$\frac{\partial p}{\partial r} = 0, \quad \frac{\partial p}{\partial \theta} = 0$$

in the r and θ directions, and

$$0 = -\frac{\partial p}{\partial z} - \rho g + \rho\nu\nabla^2 W,$$

is the z direction, where ∇^2 is the Laplacian operator in the $r - \theta$ plane. The boundary conditions are zero velocity at the wall ($r = d/2$) and at the interface ($\theta = 0$, $\theta = \pi$).

From a control-volume momentum balance, $-dp/dz = \rho_0 g$, where $\rho_0 = (\rho_T + \rho_B)/2$. Then the equation in the z direction, $0 = -(\rho - \rho_0)/\rho_0 + \nu\nabla^2 W$, which written separately for the upward going and downward going fluids becomes

$$\nu\nabla^2 W = -\frac{\Delta C}{2\rho_B} g \quad \text{(upward)}$$

$$\nu\nabla^2 W = \frac{\Delta C}{2\rho_T} g \quad \text{(downward)}.$$

To ensure symmetry we assume $(\Delta C/\rho_0) \ll 1$ and replace ρ_B and ρ_T by ρ_0 in the denominators on the right hand sides of the above equations.

Solution is same as that of a fully developed flow in pipe with a semi-circular cross section driven by a constant pressure gradient, but with the pressure gradient replaced by $g\Delta C$. The solution[5] gives the average velocity in each half of the tube as

$$\overline{W} = 0.03721(d/2)^2 \frac{\Delta C}{\rho\nu} g.$$

The flux $(-\overline{wc}) = \Delta C\overline{W}/2$ is given by

$$F_l = 0.0059 \frac{d^2(\Delta C)^2}{\rho\nu} g, \qquad (3)$$

where subscript l represents laminar flow. The relation shows the dependence of flux on various parameters and interestingly no dependence on the tube length.

In an experiment, even when the flow is HAH, because of diffusion of salt we would expect the flux to be lower than the theoretical value; the scaling will also probably change if diffusion is included. However eq. (3) gives a theoretical maximum value and can be used to non-dimensionalize experimental flux values.

Turbulent flow

We make certain assumptions based on dimensional and physical arguments to arrive at a relation for flux when the flow is turbulent. Clearly other expressions can be obtained by making different assumptions.

We assume fully developed flow – the flow is identical (in an average sense) at different Z locations, and we assume the flow is steady (again in an average sense). The first assumption will be valid if the tube is sufficiently long ($(l/d) \gg 1$) and we are far enough away from the two ends; how long and how far will have to be determined from experiments. A similar situation arises in fully developed, pressure-gradient driven turbulent pipe flow. In that case, fully developed flow is achieved about 20–50 diameters from the entrance, and in the length of the pipe where the flow is fully developed, profiles of mean velocity and, for example, profiles of the mean turbulent stresses do not change with axial distance; and the axial pressure gradient is constant.

From the fully developed flow condition we have the mean density (or concentration) gradient $d\langle C\rangle/dz$ = constant. (For the turbulent flow we use $\langle\ \rangle$ to denote time average, and prime to denote deviation from the time average.) Like the pressure gradient in the case of the pipe flow, we have the density gradient as the driving force in the vertical-tube convection flow. The independent parameters are then $d\langle C\rangle/dz$, ρ, g, and d. Viscosity and diffusivity are not considered, an usual assumption in turbulent flow.

In the vertical-tube convection case we have seen there is no mean flow, i.e. $\overline{W} = 0$. From flow visualization we have seen that when the flow is turbulent there are no two clear streams of upgoing and downgoing fluids. Thus the relevant parameters describing the flow are the flux $-\langle w'c' \rangle$, and means of the squares of fluctuating velocities ($\langle u_r'^2 \rangle$, $\langle u_\theta'^2 \rangle$ and $\langle w'^2 \rangle$) and of concentration fluctuations ($\langle c'^2 \rangle$). Prime denotes deviation from the time average.

We assume the flux to be proportional to the product of a velocity scale (say W_{turb}) and a concentration scale (say C_{turb}). These quantities may be thought of as associated with a typical fluid mass or an eddy: say a heavier fluid mass with an excess density over the ambient = C_{turb}, and moving down with a velocity W_{turb}. From the above list of independent parameters we get

$$C_{\text{turb}} = \frac{\mathrm{d}\langle C \rangle}{\mathrm{d}z} d.$$

The velocity scale can be obtained as the velocity attained by the fluid mass during free fall over some distance (a mixing length). We assume the mixing length scales as the diameter. Thus

$$W_{\text{turb}} = \left(\frac{C_{\text{turb}} g d}{\rho} \right)^{1/2} = \left(\frac{\mathrm{d}\langle C \rangle}{\mathrm{d}z} \frac{g d^2}{\rho} \right)^{1/2}.$$

Then the relation for turbulent flux is

$$F_{\text{T}} = K_{\text{T}} \left(\frac{\mathrm{d}\langle C \rangle}{\mathrm{d}z} \right)^{3/2} \left(\frac{g}{\rho} \right)^{1/2} d^2,$$

where K_{T} is a constant. Neglecting the end effects we can write $\mathrm{d}\langle C \rangle/\mathrm{d}z = (C_{\text{T}} - C_{\text{B}})/l = \Delta C/l$. Then the above expression becomes

$$F_{\text{T}} = K_{\text{T}} \frac{\Delta C^{3/2} g^{1/2} d^2}{\rho^{1/2} l^{3/2}}. \tag{4}$$

Note that the dependence on the various parameters is different from that obtained in the laminar HAH flow case (eq. (3)). In contrast to the laminar flow case, in the turbulent flow a length dependence (= $l^{-3/2}$) is present and viscosity does not enter the picture.

Experimental flux results

We compare the experimentally obtained flux of salt with the theoretically predicted flux. As mentioned earlier, from the measured salt concentration in the top tank fluid we calculate the density difference (ΔC) using relations (1) and the flux (F) using relation (2).

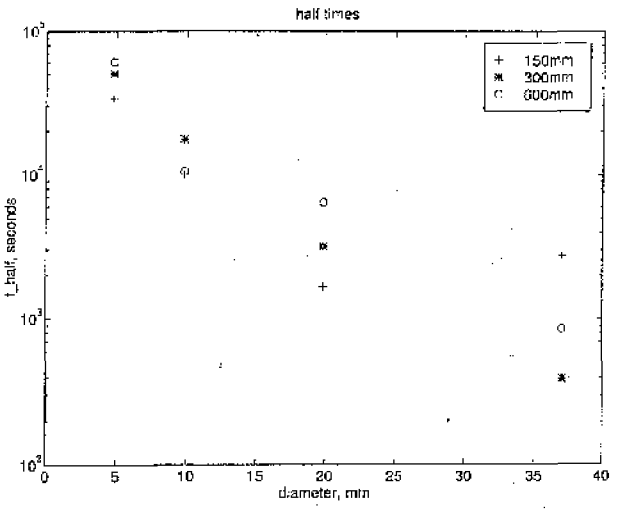

Figure 8. The half-times in the experiments with different diameter and different length tubes.

First, to give an idea of the durations of the experiments. Figure 8 shows the half-times obtained in all the experiments we have conducted. Faster mixing is obtained as the tube diameter increases, and for a given diameter the mixing is slower for a longer tube. The half time ranges from about 400 s in the case of the 36.85 mm diameter, 150 mm long tube to about 6×10^4 seconds in the case of the 4.8 mm diameter, 600 mm long tube.

Figure 9 shows for the 4.85 mm diameter cases the flux normalized by F_i (the theoretical flux for laminar HAH flow of immiscible fluids) vs Rayleigh number based on diameter. Recall in this diameter tube the flow is laminar helical type. The normalized flux values are only about 0.02 to 0.04. Clearly diffusion and mixing results in flux values much lower than theoretical values. The normalized flux value is even lower for convection in the larger diameter tubes: about 0.005 for 9.85 mm diameter tubes, and 0.001 for 36.85 mm diameter tubes.

At the other extreme is turbulent flow. We had discussed that the flow in the 36.85 mm diameter tubes appeared to be turbulent visually. We can check whether the flux in these tubes scales as predicted by the relation (4), which is for turbulent flow. Figure 10 shows, for the 300 mm and 600 mm tube lengths, the normalized flux (F/F_{T}) data plotted versus the Rayleigh number based on the diameter (K_{T} has been taken to be unity in calculating F_{T} in the plot). The data for the two diameters collapse to a reasonable extent. The normalized flux appear to be nearly constant with Rayleigh number. The constant K_{T}, in eq. (4), from the plot is about 0.5. More experiments covering a wider range of Rayleigh numbers are needed to validate and extend these results.

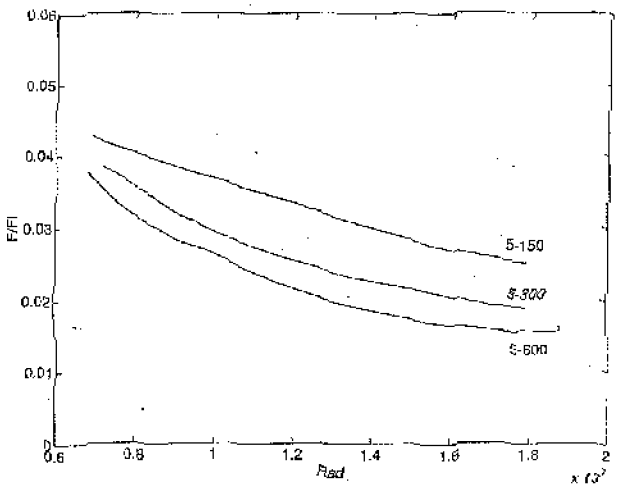

Figure 9. Plot of flux normalized by theoretical laminar flux vs Rayleigh number in the case of 4.85 mm diameter tube.

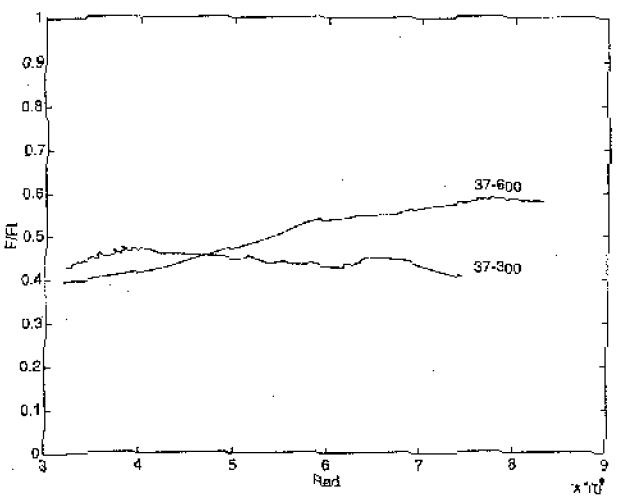

Figure 10. Plot of flux normalized by theoretical turbulent flux vs Rayleigh number in the case of 36.85 mm diameter tube.

Conclusions

We have presented preliminary results on natural convection in a vertical tube. More work is needed to resolve a number of issues; two main ones are listed below:

(i) We have given the solution for laminar *HAH* flow of fluids with zero diffusivity ($Pr \to \infty$). We need to solve for finite Prandtl numbers to realistically compare data from experiments.

(ii) We need to precisely determine the values of the transition Rayleigh numbers, when the flow switches from one type of flow to the other.

But what we think is interesting is the turbulent flow. It appears to be different from the other types of turbulent flow which we are familiar with: free shear flows like *jets, wakes, plumes, or wall bounded flows like* turbulent flow in a pipe, flow on a heated vertical wall. We have in the vertical-tube convection case a buoyancy-driven *turbulent flow with zero mean flow* and zero mean shear. Here mean refers to time average. Thus at any spatial point in the flow the time averages of the vertical velocity and of *the shear are zero. The flow is* homogeneous in the vertical direction and appears to be nearly homogeneous in the horizontal direction; because of zero mean flow the (side) *wall* seems to *just* 'contain' the flow, and does not have the overwhelming influence it has, for example, in the pressure-driven turbulent pipe flow. Besides the fluid properties and gravity, the only parameters are tube diameter and the forcing term, the density gradient.

This flow has relevance to turbulent R–B convection and during the later stages of Rayleigh–Taylor instability. In R–B convection the flow away from the walls (in the core) is similar to what is obtained in the vertical-tube convection. In R–B convection, it is well known that the wall predominantly determines the dynamics, but an issue of current interest is the interaction between the wall and core flows[5,6]. An understanding of *this interaction* may help resolve the controversy regarding the exponent in the Nusselt number–Rayleigh number correlation[3]. The vertical-tube convection can *shed light on the turbulent mixing during* Rayleigh–Taylor instability, where, as in the tube convection case, a simultaneous motion of heavy and light fluids is obtained. *Finally, the vertical-tube turbulent convection* may be similar to the decaying homogeneous buoyancy-driven turbulence studied by Batchelor *et al.*[8], using *numerical simulation, except that, in our case the turbulence* is non-decaying.

1. *Turner, J. S., Buoyancy Effects in Fluids*, Cambridge, 1972.
2. Dalziel, S. B., Linden, P. F. and Youngs, D. L., *J. Fluid Mech.*, 1999, **399**, 1–48.
3. Niamela, J. J., Skrbek, L., Sreenivasan, K. R. and Donnelly, R. J., *Nature*, 2000, **404**, 837–840.
4. Batchelor, G. K. and Nitsche, J. M., *J. Fluid Mech.*, 1993, **252**, 419–448.
5. *White, F. M., McGraw Hill*, 1991.
6. Theerthan, S. A. and Arakeri, J. H., *J. Fluid Mech.*, 1998, **373**, 221.
7. Theerthan, S. A. and Arakeri, J. H., *Phys. Fluids*, 2000, **12**, 884.
8. Batchelor, G. K., Canuto, V. M. and Chasnov, J. R., *J. Fluid Mech.*, 1991, **235**, 349–378.

ACKNOWLEDGEMENT. J.H.A. acknowledges the travel support from the Third World Academy of Sciences, and thanks the people at CIE who made the stay in Mexico during March to June, 1998 a pleasant one. We thank Murali Cholemari for help in manuscript preparation.

J. Fluid Mech. (1998), vol. 373, pp. 221–254. Printed in the United Kingdom

A model for near-wall dynamics in turbulent Rayleigh–Bénard convection

By S. ANANDA THEERTHAN
AND JAYWANT H. ARAKERI

Department of Mechanical Engineering, Indian Institute of Science, Bangalore-560 012, India

(Received 1 May 1996 and in revised form 18 May 1998)

Experiments indicate that turbulent free convection over a horizontal surface (e.g. Rayleigh–Bénard convection) consists of essentially line plumes near the walls, at least for moderately high Rayleigh numbers. Based on this evidence, we propose here a two-dimensional model for near-wall dynamics in Rayleigh–Bénard convection and in general for convection over heated horizontal surfaces. The model proposes a periodic array of steady laminar two-dimensional plumes. A plume is fed on either side by boundary layers on the wall. The results from the model are obtained in two ways. One of the methods uses the similarity solution of Rotem & Classen (1969) for the boundary layer and the similarity solution of Fujii (1963) for the plume. We have derived expressions for mean temperature and temperature and velocity fluctuations *near* the wall. In the second approach, we compute the two-dimensional flow field in a two-dimensional rectangular open cavity. The number of plumes in the cavity depends on the length of the cavity. The plume spacing is determined from the critical length at which the number of plumes increases by one. The results for average plume spacing and the distribution of r.m.s. temperature and velocity fluctuations are shown *to be in acceptable agreement with experimental results.*

1. Introduction

This paper is concerned with the near-wall dynamics of turbulent free convection over horizontal surfaces. This is taken to include steady-state convection between horizontal plates kept at constant temperatures (the classical Rayleigh–Bénard convection), unsteady convection between two horizontal plates with one of the plates insulated and convection over a horizontal plate kept in a vast expanse of stationary fluid. We do not distinguish between the near-wall dynamics that occur in these various flows. This is analogous to stating that near-wall flows in turbulent pipe flow and in the turbulent boundary layer are similar.

Turbulent free convection of this type, especially Rayleigh–Bénard convection has been studied extensively (Townsend 1959; Deardorff & Willis 1967*a*; Tanaka & Miyata 1980; Adrian, Ferreira & Boberg 1986; Castaing *et al.* 1989). See Siggia (1994) for a recent review. In this type of flow, large thermal gradients exist near the wall(s) while near isothermal conditions prevail away from the wall(s). Experimental evidence suggests the convective heat transfer near the wall(s) is either from thermals (intermittent release of hot fluid) or essentially line plumes (continuous release of hot fluid from a line) which move randomly. Away from the wall(s) rapid mixing leads to near-isothermal conditions.

J. Fluid Mech. (2005), *vol.* 526, *pp.* 245–256.
DOI: 10.1017/S0022112004002897 Printed in the United Kingdom

The multifractal nature of plume structure in high-Rayleigh-number convection

By BABURAJ A. PUTHENVEETTIL[1], G. ANANTHAKRISHNA[2] AND JAYWANT H. ARAKERI[1]

[1]Department of Mechanical Engineering, Indian Institute of Science, Bangalore, India

[2]Materials Research Center, and Centre for Condensed Matter Theory, Indian Institute of Science, Bangalore, India

garani@mrc.iisc.ernet.in

(Received July 2004)

The geometrically different planforms of near-wall plume structure in turbulent natural convection, visualized by driving the convection using concentration differences across a membrane, are shown to have a common multifractal spectrum of singularities for Rayleigh numbers in the range 10^{10}–10^{11} at Schmidt number of 602. The scaling is seen for a length scale range of 2^5 and is independent of the Rayleigh number, the flux, the strength and nature of the large-scale flow, and the aspect ratio. Similar scaling is observed for the plume structures obtained in the presence of a weak flow across the membrane. This common non-trivial spatial scaling is proposed to be due to the same underlying generating process for the near-wall plume structures.

J. Fluid Mech. (2005), vol. 542, pp. 217–249. © 2005 Cambridge University Press
doi:10.1017/S002211200500618X Printed in the United Kingdom

Plume structure in high-Rayleigh-number convection

By BABURAJ A. PUTHENVEETTIL[1] AND JAYWANT H. ARAKERI[2]

[1]Department of Applied Mechanics, Indian Institute of Technology Madras, Chennai, India
[2]Department of Mechanical Engineering, Indian Institute of Science, Bangalore, India
jaywant@mecheng.iisc.ernet.in

(Received 12 October 2004 and in revised form 29 March 2005)

Near-wall structures in turbulent natural convection at Rayleigh numbers of 10^{10} to 10^{11} at a Schmidt number of 602 are visualized by a new method of driving the convection across a fine membrane using concentration differences of sodium chloride. The visualizations show the near-wall flow to consist of sheet plumes. A wide variety of large-scale flow cells, scaling with the cross-section dimension, are observed. Multiple large-scale flow cells are seen at aspect ratio $(AR) = 0.65$, while only a single circulation cell is detected at $AR = 0.435$. The cells (or the mean wind) are driven by plumes coming together to form columns of rising lighter fluid. The wind in turn aligns the sheet plumes along the direction of shear. The mean wind direction is seen to change with time. The near-wall dynamics show plumes initiated at points, which elongate to form sheets and then merge. Increase in Rayleigh number results in a larger number of closely and regularly spaced plumes. The plume spacings show a common log-normal probability distribution function, independent of the Rayleigh number and the aspect ratio. We propose that the near-wall structure is made of laminar natural-convection boundary layers, which become unstable to give rise to sheet plumes, and show that the predictions of a model constructed on this hypothesis match the experiments. Based on these findings, we conclude that in the presence of a mean wind, the local near-wall boundary layers associated with each sheet plume in high-Rayleigh-number turbulent natural convection are likely to be laminar mixed convection type.

Planform structure and heat transfer in turbulent free convection over horizontal surfaces

S. Ananda Theerthan and Jaywant H. Arakeri
Department of Mechanical Engineering, Indian Institute of Science, Bangalore-560 012, India

(Received 11 November 1998; accepted 16 November 1999)

This paper deals with turbulent free convection in a horizontal fluid layer above a heated surface. Experiments have been carried out on a heated surface to obtain and analyze the planform structure and the heat transfer under different conditions. Water is the working fluid and the range of flux Rayleigh numbers (Ra) covered is $3\times10^7-2\times10^{10}$. The different conditions correspond to Rayleigh-Bénard convection, convection with either the top water surface open to atmosphere or covered with an insulating plate, and with an imposed external flow on the heated boundary. Without the external flow the planform is one of randomly oriented line plumes. At large Rayleigh number Ra and small aspect ratio (AR), these line plumes seem to align along the diagonal, presumably due to a large scale flow. The side views show inclined dyelines, again indicating a large scale flow. When the external flow is imposed, the line plumes clearly align in the direction of external flow. The nondimensional average plume spacing, $\mathrm{Ra}_\chi^{1/3}$, varies between 40 and 90. The heat transfer rate, for all the experiments conducted, represented as $\mathrm{Ra}_{\delta_T}^{-1/3}$, where δ_T is the conduction layer thickness, varies only between 0.1–0.2, showing that in turbulent convection the heat transfer rates are similar under the different conditions. © *2000 American Institute of Physics.* [S1070-6631(00)00903-X]

Pergamon

International Communications in Heat and Mass Transfer, Vol. 21, No. 4, pp. 561–572, 1994

0735-1933/94 $6.00 + .00

0735-1933(94)00011-5

PLANFORM STRUCTURE OF TURBULENT RAYLEIGH-BÉNARD CONVECTION

S. Ananda Theerthan and Jaywant H. Arakeri
Department of Mechanical Engineering
Indian Institute of Science, Bangalore-560 012, INDIA.

(Communicated by P.J. Heggs)

ABSTRACT

The planform structure of turbulent Rayleigh-Bénard convection is obtained from visualising a liquid crystal sheet stuck to the bottom hot surface. The bottom plate of the convection cell is Plexiglas and the top plate is glass. Water is the test liquid and the Rayleigh number is 4×10^7. The planform pattern reveals randomly moving hot streaks surrounded by cold regions suggesting that turbulent Rayleigh-Bénard convection is dominated by quasi-two-dimensional randomly moving plumes. Simultaneous temperature traces from two vertically separated thermocouples indicate that these plumes may be inclined forward in the direction of horizontal motion. The periodic eruption of thermals observed by Sparrow *et al* [3] and which forms the basis of Howard's model is not observed.

Convection in a long vertical tube due to unstable stratification – A new type of turbulent flow?

Jaywant H. Arakeri*,§, Fransisco E. Avila†, Jorge M. Dada and Ramon O. Tovar

*Department of Mechanical Engineering, Indian Institute of Science, Bangalore 560 012, India
Centro De Investigacion en Energia, Temixco, UNAM, Mexico

We present experimental results of free convection in a vertical tube due to an unstable density difference imposed between the two (open) ends of the tube. Two tanks of fluids connect the two ends of the tube with the top-tank fluid heavier than the bottom-tank fluid. We use salt mixed with water to create the density difference. The convection in the tube is in the form of relatively heavier fluid going down and lighter fluid going up simultaneously; the mean flow at any cross section of the tube is zero. Depending on the Rayleigh number we *observe different types of flow, with turbulent flow* being observed at the higher Rayleigh numbers. We believe this is a new type of turbulent flow – a nearly homogeneous, buoyancy-driven flow with zero mean shear.

FLOWS caused by buoyancy, called free or natural convection, abound in nature and engineering. The convection observed on a hot road surface in no-wind conditions is an example. Convection is generally caused by unstable stratification (for example, density increasing with height in a gravitational field). Density gradients are often caused by a temperature gradient, or a gradient of concentration of some species (e.g. salt in the oceans, water vapour in air). The dynamics in free-convection flows is mainly determined by the Rayleigh number – a measure of the ratio of buoyancy forces to diffusive effects.

Two simple configurations of free convection have been extensively studied, viz. Rayleigh–Benard convection and Rayleigh–Taylor instability. Rayleigh–Benard (R–B) convection is convection of a fluid between two horizontal plates, with the bottom plate hotter than the top plate. Because of the temperature difference, the fluid density increases from the bottom plate to the top plate. However, below a critical Rayleigh number, even though the stratification is unstable, there is no flow (convection) and heat transfer is entirely by conduction; the Rayleigh number increased beyond this critical value results in laminar convection, often in the form of *rolls, and a further increase in the Rayleigh number* leads to turbulent convection (see ref. 1).

§For correspondence (e-mail: jaywant@mecheng.iisc.ernet.in)
†Sadly, Fransisco passed away during the writing of this paper. We have fond memories of him.

Rayleigh–Taylor instability occurs when a layer of heavier fluid (say salt water) lies on top of a layer of lighter fluid (say fresh water). Dalziel *et al.*[2] report recent work on this subject. In this configuration the layers can be in equilibrium; pressure varies linearly with *depth in each of the layers. But this is unstable equilibrium*: a small perturbation of the interface increases the perturbation indefinitely with the heavier fluid trying to go down and the lighter fluid trying to go up. Some mixing between the top and bottom fluids occurs during the overturning. Eventually motion ceases and a stable density gradient is obtained. For an immiscible pair of fluids of say water over air there is negligible mixing and, eventually, the water and air layers just interchange places. One common way of doing a Rayleigh Taylor stability experiment is to have a thin plate initially separating the two fluids which is then rapidly pulled away.

In this article we describe preliminary results of free convection in a vertical tube. The setup is similar to a Rayleigh–Taylor stability setup, except that we have a long vertical tube between the tanks containing the heavier fluid at the top and the lighter fluid at the bottom (Figure 1). So essentially we look at the 'overturning' process of the two fluids through the tube. We used sodium chloride salt mixed in water to create the density difference. As in Rayleigh–Benard convection, we find different types of flow depending on the values of the parameters of the problem: the density difference, *and diameter and length of the tube. In particular, at a* high enough Rayleigh number we observe the flow to be turbulent, which we believe is a new type of turbulent flow.

Experimental setup

The experimental setup consisted of two tanks connected by a vertical tube. The top tank was open at the top and had a tapered hole in the bottom plexiglas wall to fit a rubber stopper; an appropriate sized hole was made in the stopper to snugly fit the tube. The bottom tank was closed on all sides and had a similar rubber stopper arrangement on the top wall to fit the bottom end of the tube. The rubber stoppers minimized the load

Available online at www.sciencedirect.com
SCIENCE DIRECT®
International Journal of Heat and Mass Transfer 48 (2005) 4467–4473
International Journal of HEAT and MASS TRANSFER
www.elsevier.com/locate/ijhmt

Experiments and a model of turbulent exchange flow in a vertical pipe

Murali R. Cholemari, Jaywant H. Arakeri *

Department of Mechanical Engineering, Indian Institute of Science, Bangalore 560012, India

Received 27 December 2004; received in revised form 6 April 2005
Available online 19 July 2005

Abstract

In this paper we present experimental measurements of buoyancy driven turbulent exchange flow in a vertical pipe (L/d ratios of 9–12). The flow is driven by an unstable density difference across the ends of the pipe, created using brine and distilled water. Away from either end, a fully developed region of turbulence exists with a linear density gradient. Using a mixing length model that accounts for the end effects, we obtain the turbulent scales and flux. The Nusselt number scales like the square root of the Rayleigh number ($Nu \sim Ra^{1/2}$). We give an empirical relation to quantify the end effects and hence calculate the flux of the salt (NaCl) given the aspect ratio of the pipe and the overall density difference across it.

Keywords: Turbulent mixing; Exchange flow; Mixing length model

1. Introduction

This paper is concerned with turbulent natural convection in a long vertical pipe subject to an unstable density difference across the two ends. In the present paper we model the main mechanism that drives the turbulent flow, validate the model with experimental measurements and extend it to general cases. We discuss the implications of the model on the behaviour of the flux described in terms of a Nusselt number.

Fig. 1 shows the schematic of the flow. The pipe is connected by two tanks, with the top tank fluid having higher density than the bottom tank fluid. The two fluids are miscible. The incompressibility of the fluids implies that the cross section average of the axial velocity at any instant was zero. This type of flow – where the net flow is zero—is termed 'exchange flow' [1,2].

Most of the earlier work on exchange flow [1,2] has been in the context of the fire safety of buildings. Two types of studies have been done of flow through vent(s) connecting two enclosures, one above the other. One is flow due to the combined action of pressure and density differences across the vent, for example, as discussed in Tan and Jaluria [2], and the other type is due to density difference alone, for example as studied in Epstein [1]. The present flow is related to the latter type. Epstein [1] experimentally studied the buoyancy driven exchange (counter-current) flow through single or multiple openings with both square and circular cross sections in horizontal partitions, using brine above the partition and fresh water below the partition. The openings were tubes,

* Corresponding author. Tel.: +91 80 293 3228; fax: +91 80 360 0648.
E-mail address: jaywant@mecheng.iisc.ernet.in (J.H. Arakeri).

0017-9310/$ - see front matter © 2005 Elsevier Ltd. All rights reserved.
doi:10.1016/j.ijheatmasstransfer.2005.04.025